Femtosecond x-ray pulse length characterization at the Linac Coherent Light Source free-electron laser

New Journal of Physics
The open-access journal for physics

Femtosecond x-ray pulse length characterization at the Linac Coherent Light Source free-electron laser

S Düsterer[1,12], P Radcliffe[2], C Bostedt[3], J Bozek[3], A L Cavalieri[4], R Coffee[3], J T Costello[5], D Cubaynes[6], L F DiMauro[7], Y Ding[3], G Doumy[7,8], F Grüner[9,11], W Helml[9,10], W Schweinberger[9], R Kienberger[9,10], A R Maier[9,11], M Messerschmidt[3], V Richardson[5], C Roedig[7], T Tschentscher[2] and M Meyer[2,6]

[1] FLASH at DESY, Notkestrasse 85, D-22607 Hamburg, Germany
[2] European XFEL GmbH, Albert-Einstein-Ring 19, D-22761 Hamburg, Germany
[3] Linac Coherent Light Source, 2575 Sand Hill Road, Menlo Park, CA 94025, USA
[4] Center for Free-Electron Laser Science, Notkestrasse 85, D-22607 Hamburg, Germany
[5] National Center for Plasma Science and Technology and School of Physical Sciences, Dublin City University, Dublin, Ireland
[6] Institut des Sciences Moléculaires d'Orsay, UMR 8214, CNRS–Université Paris Sud, Bâtiment 350, 91405 Orsay Cedex, France
[7] Department of Physics, The Ohio State University, Columbus, OH 43210, USA
[8] Argonne National Laboratory, Argonne, IL 60439, USA
[9] Max-Planck-Institute for Quantum Optics, Hans-Kopfermann-Strasse 1, D-85748 Garching, Germany
[10] Technische Universität München, Physik-Department E11, James-Franck-Strasse D-85748 Garching, Germany
[11] Department für Physik, Ludwig-Maximilians-Universität, Am Coulombwall 1, D-85748 Garching, Germany
E-mail: Stefan.Duesterer@desy.de

New Journal of Physics **13** (2011) 093024 (11pp)
Received 20 May 2011
Published 14 September 2011
Online at http://www.njp.org/
doi:10.1088/1367-2630/13/9/093024

[12] Author to whom any correspondence should be addressed.

Abstract. Two-color, single-shot time-of-flight electron spectroscopy of atomic neon was employed at the Linac Coherent Light Source (LCLS) to measure laser-assisted Auger decay in the x-ray regime. This x-ray-optical cross-correlation technique provides a straightforward, non-invasive and on-line means of determining the duration of femtosecond (>40 fs) x-ray pulses. In combination with a theoretical model of the process based on the soft-photon approximation, we were able to obtain the LCLS pulse duration and to extract a mean value of the temporal jitter between the optical pulses from a synchronized Ti-sapphire laser and x-ray pulses from the LCLS. We find that the experimentally determined values are systematically smaller than the length of the electron bunches. Nominal electron pulse durations of 175 and 75 fs, as provided by the LCLS control system, yield x-ray pulse shapes of 120 ± 20 fs full-width at half-maximum (FWHM) and an upper limit of 40 ± 20 fs FWHM, respectively. Simulations of the free-electron laser agree well with the experimental results.

Contents

1. Introduction

The Linac Coherent Light Source (LCLS) started lasing in the x-ray regime (0.8–8 keV) in the summer of 2009 with an unprecedented flux in the range of 10^{13} photons per pulse and controllable pulse duration from a few fs up to $\simeq$300 fs [1]. Combined with appropriate focusing optics, peak irradiance levels of more than 10^{17} W cm^{-2} are possible, extending multi-photon [2–4] and nonlinear [5] spectroscopy into the x-ray region of the electromagnetic spectrum. In addition, with temporally synchronized ultrafast lasers, new pump–probe experiments involving intense laser fields of radically different photon energies can be performed [6, 7]. In all experiments, utilizing either single-color pulses or pump-and-probe methods, the x-ray pulse duration is a pivotal parameter, and so the continuous development of reliable techniques to determine it are crucial for the full exploitation of ultrafast pulses from x-ray free-electron lasers (FEL). Hence, we set out to measure the LCLS pulse duration in a two-color gas phase cross-correlation experiment, which meets the desirable criteria of being non-invasive and potentially employable as an on-line diagnostic. Our focus here is on the measurement of x-ray pulse durations larger than 40 fs. Experiments to determine pulse durations shorter than 5 fs require a completely different methodology and will be published separately [8]. In addition to the pulse length, the technique reported here can reveal and quantify the timing jitter of the FEL with respect to an external synchronized optical laser, a parameter especially important for time-resolved pump-and-probe experiments.

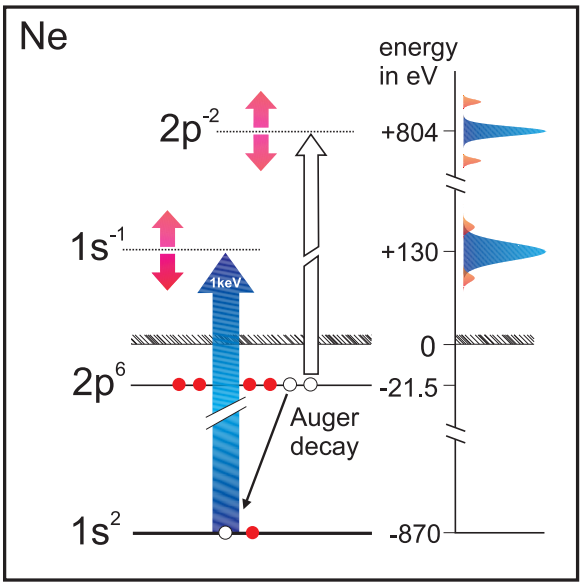

Figure 1. Simplified energy-level diagram and two-color excitation schemes for atomic Ne. Note that for the Auger process, ejection of the 2p electron in the Ne^+ ion requires 44.2 eV.

A two-color process, sensitive to the separation between x-ray and near-infrared (NIR) laser pulses, is shown in figure 1. When electrons generated by the x-ray photoionization of atoms emerge into an intense NIR field, they exchange photons with the field causing *sidebands* to appear in the electron kinetic energy spectrum. This leads to new lines separated from the main photoelectron line by multiples of $\hbar\omega_{\mathrm{NIR}}$ [9, 10]. However, in the soft x-ray energy regime (1 keV) the photon energy of the NIR laser (1.55 eV) is substantially less than the natural bandwidth of the FEL (0.5–1% full-width at half-maximum (FWHM)). Therefore, it is advantageous to use the free electrons created in an Auger decay process following inner-shell excitation (resonant Auger decay) or direct ionization (normal Auger decay). Here the kinetic energy and spectral width of the Auger lines are completely independent of the ionizing x-ray pulse as long as the photon energy is high enough to create the inner-shell vacancy and to avoid near-threshold phenomena. All perturbing effects of wavelength jitter affect only the photo- and not the Auger electron. However, for a fast enough ($\ll$5 fs) decay the time structure of the ionizing x-ray pulse is directly mapped onto the Auger electrons. This effect of the NIR laser, coined laser-assisted Auger decay (LAAD), was observed first for the argon $L_{23}M_{23}M_{23}$ Auger electrons centered at 205 eV [11], which were investigated indeed earlier than the sidebands on the photoelectron lines for the determination of x-ray pulse duration [9, 10]. In neon the inner-shell photoionization step Ne $1s^2 + \hbar\omega_{\mathrm{FEL}} \rightarrow$ Ne $1s^1 + \epsilon l$ is followed by the filling of the Ne K-shell core–hole vacancy, which results in the Auger decay of an electron with a kinetic energy of 804.3 eV [12]. Due to the narrow, fixed spectral bandwidth of the Auger line (0.23 eV FWHM), corresponding to the very short lifetime of 2.4 fs, the sidebands in the two-color Auger spectrum will be, in principle, better separated than in the case of the dressed Ne $1s^{-1}$ photoelectron line. Hence, we use LAAD as a cross-correlation signature to determine the x-ray pulse duration for two different settings of the accelerator, corresponding to nominal electron bunch durations of 75 and 175 fs, respectively.

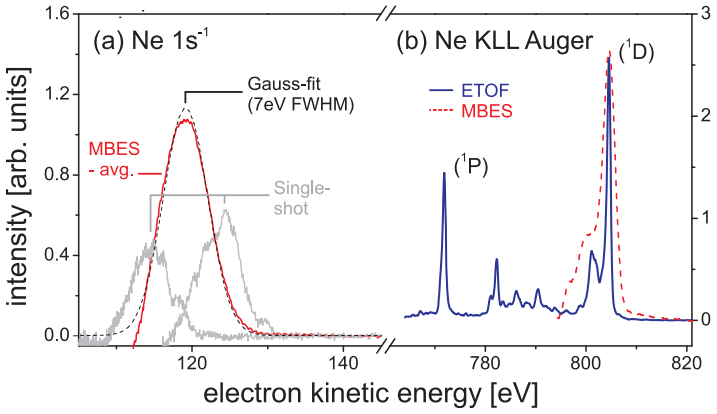

Figure 2. Photo- and Auger-electron spectra from neon after irradiation by 1 keV LCLS pulses. (a) Averaged Ne $1s^{-1}$ photo-line situated at ∼120 eV: the experimental line is described by a Gaussian profile of 7 eV FWHM corresponding to the natural FEL bandwidth. Single-shot spectra (not to scale) highlight the shot-to-shot energy jitter of the FEL. (b) Ne KLL Auger spectrum obtained with the MBES averaged over 200 shots: the line width of the main ^{1}D line is 3 eV FWHM (dashed line). The full Auger spectrum recorded with an ETOF spectrometer in the HFP chamber is shown for comparison (solid line).

2. Experimental setup

In this work, we used the diagnostic chamber of the atomic, molecular and optical (AMO) end station [13]. It comprises a magnetic bottle electron spectrometer (MBES), a gas inlet providing an effusive gas flow in the interaction region and various beam imaging tools. The photo- and Auger electrons resulting from the interaction of neon gas with the x-ray beam are analyzed by the MBES with an angular acceptance of approximately 0.8 sr (30° half-angle) at electron kinetic energies around 0.8 keV [14]. The performance of the MBES is briefly demonstrated in figure 2, which shows the main features of the electron spectrum recorded after the exposure of Ne atoms to x-ray pulses with a mean photon energy of 990 eV. In the lower kinetic energy region, the main Ne $1s^{-1}$ photo-line appears at 120 eV. The spectrum shown in figure 2(a) is an average over 200 single-shot spectra and the line profile is well represented by a Gaussian fit of 7 eV FWHM. This value is mainly determined by the natural bandwidth of the LCLS. To demonstrate the photon energy fluctuations from shot to shot, two single-shot spectra are shown in figure 2(a), demonstrating the single-shot capability of the MBES. This is a necessary prerequisite for experiments with the strongly varying temporal, spatial and spectral beam conditions inherent in FEL radiation.

In the energy region around 770–810 eV, the Ne KLL Auger spectrum is presented (figure 2(b)). For the MBES, only the most intense line around 804 eV kinetic energy is shown, corresponding to the transition to the Ne^{2+} $3p^4$ ^{1}D final state. For comparison, we also display a spectrum recorded with the high-resolution electron time-of-flight (ETOF) spectrometer situated in the AMO high-field physics (HFP) chamber, demonstrating that no additional structures show up on the high-energy side of the ^{1}D line. Since the width of the Auger lines does not depend on the energy width of the exciting photon pulse or on its spectral jitter, the spectra allow us to determine the energy resolution of the analyzers. An electron energy

resolution of 0.4% (∼3.0 eV FWHM) was achieved with the MBES by carefully optimizing the retardation voltages and acceptance geometry of the spectrometer [14]. Despite this good resolution, individual sidebands could not be resolved; however, it was sufficient to reliably simulate the data (see figure 4). The high-resolution spectrum obtained by using the ETOF is measured with an energy resolution $\Delta E/E$ of the order of 0.1%. However, the narrow angular acceptance of the ETOF (0.007 sr) does not permit single-shot acquisition with sufficient statistics.

For the measurements presented here, the LCLS was operated in the 250 pC (charge per electron bunch) mode at a pulse repetition frequency of 30 Hz and an electron beam energy of 4.7 GeV ($\hbar\omega_{\mathrm{FEL}} = 1.0$ keV nominal). Two different compression settings of the accelerator were used in order to achieve electron pulse lengths of $\tau_{\mathrm{el}} = 75$ and 175 fs, resulting in peak currents of 1.79 and 0.91 kA, respectively [1]. The total x-ray energy per pulse typically varied from 0.5 to 2 mJ, with fluctuations of 20% (FWHM) about the mean energy observed from the pulse energy distribution, which was monitored by a photon flux detection setup integrated into the beam line [15]. Adaptive focusing mirrors, arranged in a Kirkpatrick–Baez geometry, were adjusted to produce a FEL spot diameter of about 60 μm in the interaction region. The NIR laser system delivered a pulse of duration $\tau_{\mathrm{NIR}} = 100$ fs (FWHM) at a central wavelength of 800 nm and a pulse energy of 200 μJ with a pulse repetition frequency of up to 360 Hz. The last turning mirror for the laser, located on the FEL beam axis inside the vacuum chamber, has a 2 mm diameter hole in its center, through which the focused FEL beam was directed. An NIR spot of 300 μm FWHM ensured good spatial overlap of the NIR and x-ray beams and yielded focal intensities of the NIR laser $I_{\mathrm{NIR}} \sim 10^{12}$ W cm^{-2} in the interaction region. Hence, the experiment was quite insensitive to shot-to-shot jitter in the spatial overlap due to the beam pointing fluctuations in either the Ti-sapphire laser or the FEL. The spatial overlap between the LCLS and NIR laser beams was controlled by introducing a Ce:YAG viewing screen into the region of interaction and adjusting the NIR laser beam steering such that both spots were overlapped. Coarse timing (with a precision of ∼30 ps) was achieved with a fast photodiode. Final optimization of the temporal and the spatial overlap was done by monitoring the LAAD yield itself. Details of the laser system and its synchronization to the LCLS accelerator can be found in [6].

3. Results and discussion

A set of electron spectra recorded as a function of the relative delay time (in the range of ±1 ps) between the NIR and x-ray pulses is shown in figure 3. For clarity, only the main Auger line and the part of the spectrum lying to its high-energy side are displayed. Each spectrum represents the acquisition of many single-shot spectra (∼10^3), which were sorted *a posteriori* into 50 fs time bins, according to the LCLS phase cavity electron arrival time monitor and averaged [6]. In the cross-correlation region, the action of the NIR field causes a strong redistribution of the Auger electrons, resulting in the evolution of a prominent feature at higher kinetic energies and a concomitant intensity reduction of the main line at 804.3 eV. The total electron yield remains constant, as the NIR field does not contribute to the primary ionization process. Since the current setup cannot resolve individual sidebands, the LAAD process appears as a rather coarse broadening of the Auger line. Nevertheless, we can infer from the cut-off in the kinetic energy spectrum at maximum overlap ($\tau_{\delta t} = 0$) that up to 15 NIR photons are absorbed from the dressing field. This is in good agreement with the so-called Simpleman model [11]. Here,

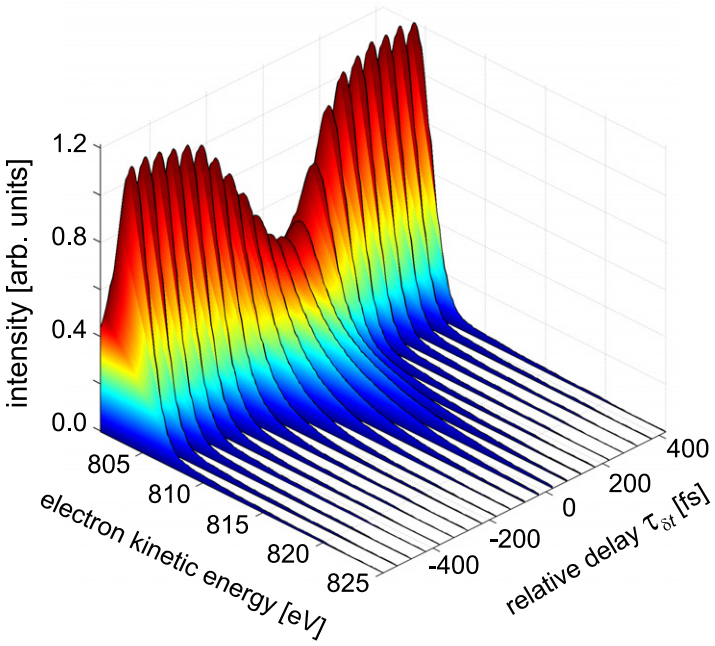

Figure 3. Neon Auger electron energy spectra as a function of the relative delay time $\tau_{\delta t}$ between the NIR ($\tau_{\mathrm{NIR}} = 100$ fs) and the x-ray pulses ($\tau_{\mathrm{el}} = 75$ fs). Around the relative zero point, the strong depletion and broadening of the main line corresponds to LAAD.

the final kinetic energy U of an electron introduced into a moderate NIR field (with wavelength λ_{NIR}) with an intensity I_{NIR} is given by

$$U = U_a - \sin(\phi_b)\cos(\theta_b)\sqrt{8U_aU_{\mathrm{p}}}. \tag{1}$$

ϕ_b is the phase of the NIR field at the instant of ionization, θ_b is the angle between the light polarization and the initial velocity of the electron at birth and U_a is the initial kinetic energy. U_{p} is the instantaneous ponderomotive energy at the moment of birth:

$$U_{\mathrm{p}}[\mathrm{eV}] = 9.33 \times 10^{-14} \times \lambda^2_{\mathrm{NIR}}[\mu\mathrm{m}^2] \times I_{\mathrm{NIR}}[\mathrm{W\,cm}^{-2}]. \tag{2}$$

For $\lambda_{\mathrm{NIR}} = 0.8\,\mu$m and $I_{\mathrm{NIR}} = 1.2 \times 10^{12}\,\mathrm{W\,cm}^{-2}$, U_{p} results in 0.07 eV. This, when substituted into equation (1), gives a maximum energy $U \simeq 826$ eV or, in other words, the absorption of about 14 NIR photons from the field. This is in excellent agreement with the experimental findings shown in figure 3. For a given intensity and wavelength of the NIR laser, U scales with the square root of the initial kinetic energy U_a. Hence, compared with two-color processes previously observed at extreme ultraviolet wavelengths, the large number of sidebands observed here at low NIR intensity is a direct consequence of the high kinetic energy of the Auger electron [10, 16].

In figure 4, several single-shot electron spectra, recorded at the nominal maximum temporal overlap between the x-ray and NIR pulses, are shown. The strong shot-to-shot variation in the LAAD component demonstrates clearly the timing jitter in the synchronization and highlights the usefulness of the LAAD effect as a sensitive monitor of the temporal overlap of the pulses. This is even more evident when the experimental line profiles are modeled with a simplified analytical model based on the so-called soft-photon approximation (SPA), allowing us to

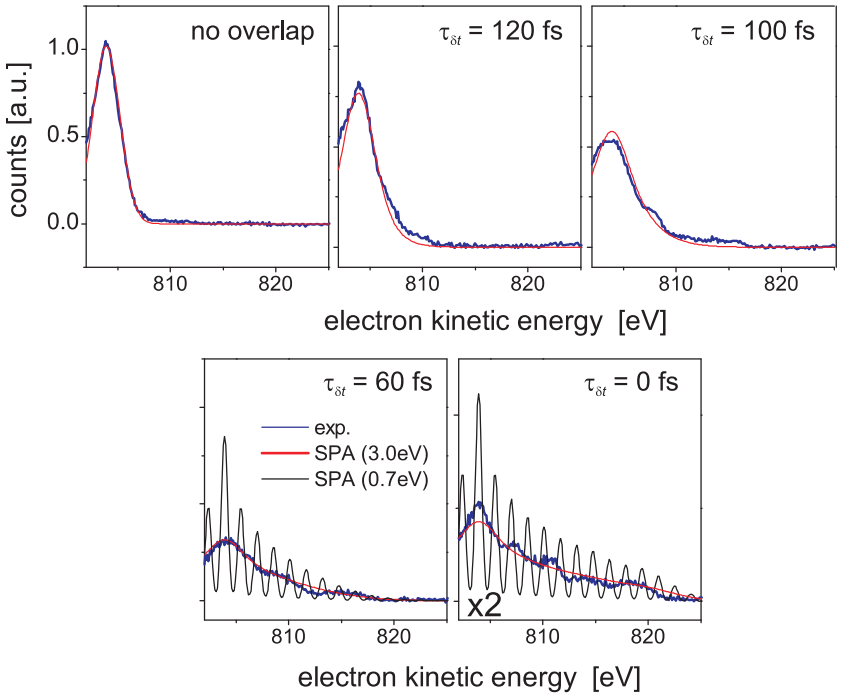

Figure 4. Selected single-shot (blue line) LAAD spectra ($\tau_{el} = 75$ fs) and corresponding results from the SPA. The SPA spectra were calculated for $\tau_{NIR} = 100$ fs FWHM ($I_{NIR} = 1200\,GW\,cm^{-2}$) and for $\tau_{x\text{-}ray} = 40$ fs. Shown are spectra simulated with the experimental energy resolution of 3.0 eV FWHM (red line) as well as with 0.7 eV FWHM (gray line in the lower two figures) in order to demonstrate the underlying sideband structure, which is otherwise washed out by the energy resolution of the MBES.

simulate the LAAD spectrum [17]. In general, the SPA gives excellent agreement with LAAD data and can match the more elaborate non-perturbative methods such as the time-dependent Schrödinger equation (TDSE) when the electron kinetic energy is large compared with the dressing photon energy [17, 18].

The simulated LAAD spectra are defined by four parameters: the NIR laser pulse duration, τ_{NIR}, and intensity I_{NIR}, the FEL pulse duration (and shape) $\tau_{x\text{-}ray}$ and, finally, the relative temporal delay between the two pulses $\tau_{\delta t}$. The NIR pulse width was measured with an auto-correlator to be $\tau_{NIR} = 100$ fs (FWHM with Gaussian profile). Monitoring the pulse energy and the focal spot size, a peak intensity of $I_{NIR} = 1.2 \times 10^{12}\,W\,cm^{-2}$ was estimated. The average jitter on the relative temporal delay was determined using two independent approaches. First, we analyzed the cross-correlation width for FEL pulse duration settings of $\sim$20 fs or shorter pulses (the so-called 20 pC mode). Here the x-ray pulse duration is negligible in the determination of the correlation width, which is only determined by the optical pulse duration and the jitter. Knowing the laser pulse duration, we obtained from the LAAD analysis a value $\tau_{jitter} = (140 \pm 20)$ fs FWHM, including the electron pulse arrival time correction data from the phase cavity measurement [6]. An alternative approach is to determine the jitter from the single-shot spectra by fitting the data as shown in figure 4 with the SPA simulation. Here the delay between the NIR and the x-ray pulse was used as a fit parameter, yielding a list

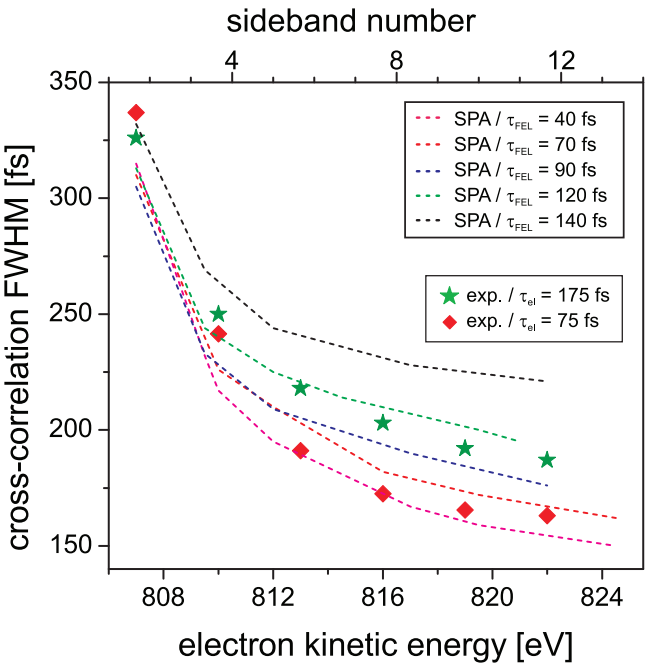

Figure 5. Comparison of experimentally obtained cross-correlation widths with those calculated within the SPA using the following parameters (in FWHM): $\tau_{\text{x-ray}} = 40$–140 fs, $\tau_{\text{NIR}} = 100$ fs and $\tau_{\text{jitter}} = 140$ fs, $I_{\text{NIR}} = 1.2 \times 10^{12}$ W cm^{-2}.

of time delays and thus the average jitter. The calculation was performed with x-ray pulse durations $\tau_{\text{x-ray}} = 75$ fs (FWHM), as the upper limit for the expected x-ray pulse duration, and also for $\tau_{\text{x-ray}} = 40$ fs FWHM, as determined in this paper (see below). The jitter determined for both pulse durations agrees within the error bars with the value determined via the cross-correlation approach, i.e. $\tau_{\text{jitter}} = (140 \pm 20)$ fs FWHM. We note that the jitter depends on many parameters and is sensitive to minor changes in the settings of the feedback electronics, the beam transport optics and associated systems, and the distribution system and mechanical vibrations. Thus, the jitter may vary significantly and other investigators have reported values approaching 300 fs (FWHM) [6].

As discussed above, under our experimental conditions LAAD is a highly nonlinear multi-photon effect, which has a strong dependence on the driving NIR laser intensity. Thus, the cross-correlation width at these intensities is no longer a direct measure of the cross-correlation of the laser and the x-ray pulse. Therefore, quantitative information about the x-ray pulse duration $\tau_{\text{x-ray}}$ can only be extracted by comparing the LAAD features to the theoretical model. In order to simulate the experimental data using the soft-photon model the NIR laser pulse, modeled as a Gaussian temporal profile, is divided into 5 fs time windows with constant intensity. Within each such segment the resulting LAAD spectrum, including all amplitudes from 30 sidebands, is calculated successively. Since the NIR laser does not contribute to the initial photoionization step, the relative amplitude of each segment spectrum is given by the FEL photon flux only. Here, the approximate pulse shapes from the FEL simulation were used as input (see below). In the final step, the component spectra were summed to represent an experimental single-shot spectrum. To simulate the full experimental set as shown in figure 3, a delay scan from -500 fs to $+500$ fs in 10 fs steps was used. For each time step, 50 single-shot spectra were accumulated and a random additional temporal time difference was introduced to simulate the time jitter.

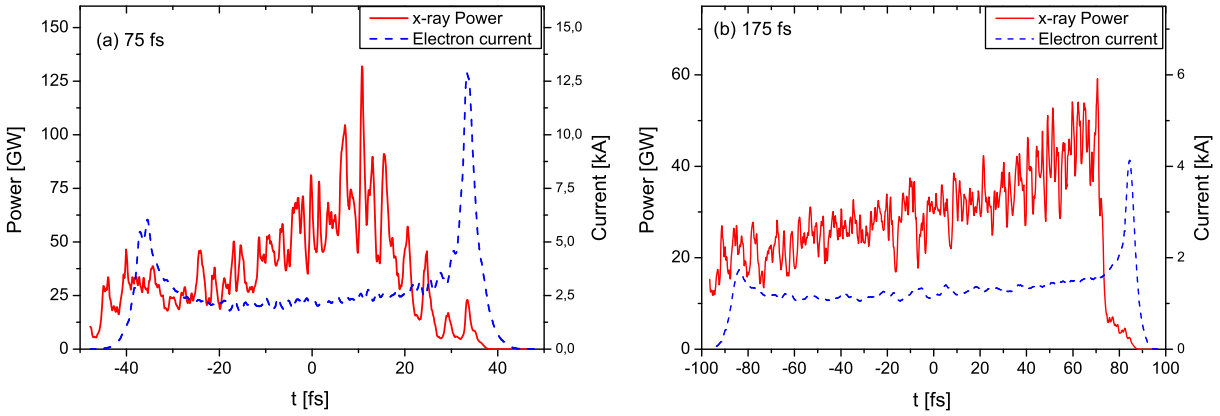

Figure 6. The temporal profile of GENESIS-simulated FEL pulses. The FEL radiation power in GW (red line) and the electron current profile (blue curve) are shown for (a) $\tau_{el} = 75$ fs and (b) $\tau_{el} = 175$ fs. The bunch head is on the left.

According to the experimental findings, a Gaussian time delay distribution with an FWHM of 140 fs was used.

Shown in figure 5 is a comparison of the experimental cross-correlation widths, obtained by a projection along the time axis (cf figure 3) and the results of the SPA simulation. As expected, the calculated widths are strongly dependent on the NIR intensity; that is, for low-order sidebands they are considerably greater than for higher sidebands. The experimental widths extracted from the cross-correlation curves recorded with an electron pulse duration of $\tau_{el} = 75$ and 175 fs, respectively, show the same general behavior as a function of kinetic energy and can be described well by the SPA simulation. A closer inspection of figure 5 shows that the measured pulse durations for $\tau_{el} = 75$ fs point to an actual x-ray pulse width of $\tau_{x\text{-}ray} = (40 \pm 20\,\text{fs})$, which is also in agreement with indirect measurements presented in [4]. The experimental values obtained for $\tau_{el} = 175$ fs are best described by a pulse of width $\tau_{x\text{-}ray} = 120 \pm 20$ fs (FWHM). These results of the LAAD cross-correlation analysis are further corroborated by a set of FEL simulations using the GENESIS code [19]. The radiation power profiles shown in figure 6 are averaged over 50 Genesis runs using random initial shot noise. For the experimental parameters chosen, GENESIS predicts for an electron pulse duration of $\tau_{el} = 75$ fs an almost Gaussian-like x-ray pulse with $\tau_{x\text{-}ray} \simeq 40$ fs (FWHM) and for $\tau_{el} = 175$ fs a more triangular-like x-ray pulse with a total width of 170 fs (120 fs FWHM). It is also noteworthy that a 120 fs FWHM Gaussian x-ray pulse yields results similar to a triangular pulse. This is due to the fact that the jitter and optical pulse duration dominate the cross-correlation and thus the x-ray pulse shape cannot be determined directly. In addition to the good agreement between experimentally determined and simulated values for nominal pulse durations of 75 and 175 fs, our measurements for the longest (nominal $\tau_{el} = 300$ fs) pulses yield a much shorter pulse duration of only $\sim$120 fs FWHM, whereas the GENESIS simulation suggests a 300 fs long x-ray pulse. Further studies are needed to resolve this discrepancy for the longest FEL pulses.

4. Conclusion

In conclusion, we have analyzed the pulse width and timing performance of the LCLS x-ray FEL using single-shot time-of-flight electron spectroscopy to perform an x-ray-optical cross-correlation measurement at the LCLS. We have investigated for the first time the two-color

LAAD process in the x-ray region, demonstrating good agreement between the experimental and simulated LAAD spectra. Also, the results show that two-color processes, known from extreme ultraviolet FEL sources [16], can be directly transferred to the x-ray regime and are even more pronounced at the resulting electron energies. The corresponding cross-correlation analysis shows for the tested electron pulse durations of $\tau_{el} = 75$ and 175 fs that the effective x-ray pulses (in FWHM) are shorter than the electron pulses, and values of $\tau_{x\text{-}ray} = 40$ and 120 fs (FWHM), respectively, have been found. Furthermore, our analysis of the single-shot statistics demonstrates that synchronization between the NIR and x-ray lasers can be achieved with a precision of at least 140 fs (FWHM). The LAAD effect can in principle be observed for any Auger line independently of the target atom and the precise photon energy of the x-ray pulse as long as the core vacancy in the atom can be created. Therefore, the method can be applied over a wide range of photon energies by selecting the most adequate Auger transition. However, the decreasing cross-section for photoionization of a given core hole with increasing photon energy might favor the choice of a particular Auger transition, for example Ar LMM and Kr LMM in the case of lower (>250 eV) and higher (>1800 eV) photon energies, respectively. Finally, we note that with shorter optical pulses and a lower jitter, this cross-correlation method has the potential to provide accurate on-line information not only on the width of shorter x-ray pulses (10–40 fs), but also on the (average) pulseform of the LCLS radiation itself.

Acknowledgments

Portions of this research were carried out at the Linac Coherent Light Source (LCLS) at the SLAC National Accelerator Laboratory. LCLS is funded by the US Department of Energy, Office of Basic Energy Sciences. We also acknowledge the dedication and hard work of the scientific and technical teams at LCLS, in particular the machine operators. We thank P Hayden and W Li for assistance with the simulation program. JTC acknowledges support from SFI PI grant no. 07/IN.1/I1771 and the HEA PRTLI IV INSPIRE program. RK acknowledges funding from an ERC Starting Grant. ARM acknowledges financial supported from the Munich-Centre of Advanced Photonics. DC and MM acknowledge financial support from the CNRS within the PEPS-SASELEX program. LFD and CR acknowledge support from the NSF and Hagenlocker chair and GD acknowledges funding from the US Department of Energy, Office of Basic Energy Sciences (DE-AC02- 06CH11357).

References

[1] Emma P *et al* 2010 *Nat. Photonics* **4** 641
[2] Hoener M *et al* 2010 *Phys. Rev. Lett.* **104** 253002
[3] Berrah N *et al* 2010 *J. Mod. Opt.* **57** 1015
[4] Young L *et al* 2010 *Nature* **466** 56
[5] Doumy G *et al* 2011 *Phys. Rev. Lett.* **106** 083002
[6] Glownia J *et al* 2010 *Opt. Express* **18** 17620
[7] Cryan J P *et al* 2010 *Phys. Rev. Lett.* **105** 083004
[8] Helml W *et al* submitted
[9] Glover T E, Schoenlein R W, Chin A H and Shank C V 1996 *Phys. Rev. Lett.* **76** 2468
[10] Meyer M *et al* 2006 *Phys. Rev.* A **74** 011401

[11] Schins J M, Breger P, Agostini P, Constantinescu R C, Muller H G, Grillon G, Antonetti A and Mysyrowics A 1994 *Phys. Rev. Lett.* **73** 2180
[12] Southworth S H, Kanter E P, Krässig B, Young L, Armen G B, Levin J C, Ederer D L and Chen M H 2003 *Phys. Rev.* A **67** 062712
[13] Bozek J 2009 *Eur. Phys. J.* **169** 129
[14] Roedig C *et al* submitted
[15] Hau-Riege S P, Bionta R M, Ryutov D D and Krzywinski J 2008 *J. Appl. Phys.* **103** 053306
[16] Meyer M, Costello J T, Düsterer S, Li W B and Radcliffe P 2010 *J. Phys. B: At. Mol. Opt. Phys.* **43** 194006
[17] Maquet A and Taïeb R 2007 *J. Mod. Opt.* **54** 1847
[18] Meyer M *et al* 2008 *Phys. Rev. Lett.* **101** 193002
[19] Reiche S *et al* 1999 *Nucl. Instrum. Methods* A **429** 243